Performance of Steel Moment Connections under a Column Removal Scenario. I: Experiments

H. S. Lew, Ph.D., P.E., F.ASCE[1], Joseph A. Main, Ph.D., A.M.ASCE[2], Stephen D. Robert, A.M.ASCE[3], Fahim Sadek, Ph.D., M.ASCE[4], and Vincent P. Chiarito, P.E., M.ASCE[5]

Abstract: This paper presents an experimental study of two full-scale steel beam-column assemblies, each comprising three columns and two beams, to (1) define their response characteristics under a column removal scenario, including the capacity of the beams and their connections to carry loads through catenary action, and (2) provide experimental data for validation of beam-to-column connection models for assessing the robustness of structural systems. The assemblies represent portions of the exterior moment-resisting frames of two ten-story steel frame buildings. One test specimen had welded unreinforced flange, bolted web connections, and the other had reduced beam section connections. When subjected to monotonically increasing vertical displacement of the unsupported center column, both specimens exhibited an initial elastic response dominated by flexure. With increased vertical displacement, the connections yielded, and axial tension developed in the beams. The axial tension in the beams increased until the connections failed under combined bending and axial stresses. The test results show that the rotational capacities of both connections under monotonic column displacement are about twice as large as those based on seismic test data.

CE Database subject headings: Buildings; Connections; Full-scale tests; Progressive collapse; Seismic design; Steel structures.

[1] Senior Research Structural Engineer, Engineering Laboratory, National Institute of Standards and Technology, Gaithersburg, MD 20899-8611, hsl@nist.gov
[2] Research Structural Engineer, Engineering Laboratory, National Institute of Standards and Technology, Gaithersburg, MD 20899-8611, joseph.main@nist.gov
[3] Research Structural Engineer, U.S. Army Engineer Research and Development Center, Vicksburg, MS, Stephen.D.Robert@erdc.usace.army.mil
[4] Leader, Structures Group,, Engineering Laboratory, National Institute of Standards and Technology, Gaithersburg, MD 20899-8611, fahim.sadek@nist.gov
[5] Research Structural Engineer, U.S. Army Engineer Research and Development Center, Vicksburg, MS, Vincent.P.Chiarito@erdc.usace.army.mil

Introduction

Current design standards and guidelines in the U.S., including the American Society of Civil Engineers Standard 7 (ASCE 2010, Section C1.4), the guidelines of the U.S. General Services Administration (GSA 2003), and the Unified Facilities Criteria (UFC) 4-023-03 of the Department of Defense (DOD 2009), provide guidance to prevent disproportionate collapse. Disproportionate collapse (also known as progressive collapse) occurs when an initial local failure spreads progressively, resulting in total collapse or collapse of a disproportionately large part of a structure. In current guidance documents, the primary approach for assessing resistance to disproportionate collapse is the alternate path method, in which analysis is performed to assess whether the structural system can withstand the removal of selected columns or other vertical load-bearing elements without collapse. Because of the large displacements and rotations that can develop in such scenarios, the rotational capacity of beam-to-column connections is a critical factor in assessing whether collapse can be averted.

Currently, design and evaluation of steel structures for disproportionate collapse resistance are based primarily on acceptance criteria obtained from seismic research (e.g., FEMA 2000a). While extensive testing has been conducted to characterize the performance of steel beam-to-column connections under seismic loading (e.g., FEMA 2000b), the demands imposed on connections under column removal scenarios differ significantly from those under seismic loading. While seismic loading is cyclic in nature, column removal scenarios result in monotonic loading of the connections. In addition, while seismic loading subjects connections primarily to bending, column removal scenario can subject connections to a combination of bending moment and axial tension, due to the development of catenary action. Limited testing of steel beam-to-column connections under column removal scenarios has been conducted, with

examples including testing of two different moment connections (Karns et al. 2007), testing of single-plate shear connections (Thompson 2009), and testing of WT connections (Friedman 2009).

The National Institute of Standards and Technology (NIST) is conducting a comprehensive research program to study the vulnerability of structures to disproportionate collapse and to develop improved guidance to reduce such vulnerability. As part of this research, prototype 10-story buildings with various structural systems have been designed, including steel frame, cast-in-place concrete frame, and precast concrete frame buildings. Subassemblies representing portions of the framing system of these prototype buildings have been tested at full scale under simulated column removal. An important objective of this testing is to provide experimental data for validation of finite element models that have been developed to represent nonlinear behavior and failure modes of the connections. Reduced finite element modeling approaches developed as part of this effort are being implemented in three-dimensional models for assessing the vulnerability of complete structural systems to disproportionate collapse. Sadek et al. (2011) present an overview of NIST research in this area, summarizing selected experimental and computational results for both steel and cast-in-place concrete moment frames.

This paper describes full-scale testing of two steel beam-column assemblies, each comprising three columns and two beams and representing part of the second floor framing of a ten-story steel frame building. The specimens are subjected to monotonically increasing vertical displacement of the unsupported center column to observe their behavior under a simulated column removal scenario, including the development of catenary action in the beams. Each test is terminated upon reaching a collapse mechanism of the assembly. The rotational capacities of

the connections based on these tests are found to be nearly twice the rotational capacities that are predicted on the basis of seismic test data. A companion paper (Sadek et al. 2012) presents finite-element based analyses of the test specimens, including comparisons with the full-scale test results.

While the focus of this study is on the performance of the bare steel framing system, the composite floor system in a real building would undoubtedly contribute to the collapse resistance of the structure under column removal scenarios. Contributions of the floor system would include composite action of the floor slab and beams, the development of tensile membrane forces in the slab, and lateral restraint of the columns. The influence of such effects is currently being studied by NIST researchers, using the reduced models described in the companion paper (Sadek et al. 2012) to analyze the three-dimensional behavior of the entire structural systems of the prototype buildings.

Description of Prototype Building Designs

NIST developed the overall configuration and dimensions of the prototype buildings to be considered in this research program. For simplicity of design and analysis, a 10-story building with rectangular plan for office occupancy was chosen as the prototype building. For the study reported herein, two steel frame buildings were designed, each having plan dimensions of 30.5 m × 45.7 m, with five bays in both the longitudinal and transverse directions. The detailed design of the building was carried out by a consulting engineering firm (Liang et al. 2008).

To examine the effectiveness of seismic design and detailing, including seismic connections, in resisting disproportionate collapse, one building was designed for Seismic Design Category C (SDC C) and the other for SDC D. The lateral loads are resisted by exterior moment-resisting frames. All interior frames were designed to support gravity loads only. The SDC C building,

designed for Atlanta, Georgia, used intermediate moment frames [IMFs, see Section 10 of AISC (2002)] for the lateral load resisting system, while the SDC D building, designed for Seattle, Washington, used special moment frames [SMFs, see Section 9 of AISC (2002)]. Plan views of the two buildings are shown in Fig. 1, with the locations of the moment frames indicated.

The buildings were designed according to the American Society of Civil Engineers 7-02 standard (ASCE 2002). The material standards used in the design of the members and their connections were referenced in ASCE 7-02, including the American Institute of Steel Construction (AISC) "Load and Resistance Factor Design Specification for Structural Steel Buildings" (AISC 1999) and the AISC "Seismic Provisions for Structural Steel Buildings" (AISC 2002). Connections used in the moment frames were selected from the prequalified steel connections in FEMA 350 (FEMA 2000a), which was the available standard at the time. Welded unreinforced flange, bolted web (WUF-B) connections were used for the IMFs (SDC C) and reduced beam section (RBS) connections were used for the SMFs (SDC D). ASTM A992 structural steel (F_y = 344.8 MPa) was used in all beams, columns, and doubler plates in the panel zones. ASTM A36 steel (F_y = 248.2 MPa) was used for the shear tabs and continuity plates at beam-column connections. For the bolted moment connections, ASTM A490 high strength bolts were used.

Moment Connections

For the beam-column assembly tests, two-span beams connected to three columns were selected from the second floor of the moment resisting frames. The span length of the beams (center-to-center of columns) was 6.10 m. The beams selected from the SDC C building were W21x73 sections and were connected to W18x119 columns using WUF-B connections, while the beams selected from the SDC D building were W24x94 sections and were connected to W24x131

columns using RBS connections. While the behavior of the WUF-B and RBS connections have been extensively studied under seismic loading, their performance under the monotonic loading conditions expected in disproportionate collapse scenarios, in which connections are subjected to monotonically increasing combined bending and tension, has not been previously studied and is the subject of this paper.

Welded Unreinforced Flange, Bolted Web (WUF-B) Connection

The WUF-B connection is similar to the connections commonly used prior to the 1994 Northridge earthquake. After significant research (FEMA 2000b), it was determined that with several improvements and appropriate quality assurance, this connection can perform reliably. Improvements over the typical pre-Northridge connections included: using weld metal with appropriate toughness; removing weld backing from bottom-beam-flange-to-column-flange welds, back-gouging and addition of a reinforcing fillet weld; using improved weld access hole shape and finish; and applying better weld quality control and quality assurance. FEMA 355D (FEMA 2000b) provides extensive information on the testing and performance of the WUF-B connections (pre- and post- Northridge) under seismic loading.

The inter-story drift angle or rotational capacity of the WUF-B connection specified in FEMA 350 was based on a statistical analysis of results from cyclic tests of full-scale connection assemblies. The rotational capacity corresponding to collapse prevention θ_U, characterized by the inability of the connection to maintain its integrity under gravity loading, was estimated for the WUF-B connection as:

$$\theta_U = 0.060 - 0.0006 d_b \quad (1)$$

where d_b is the beam depth in inches. For the W21x73 beam section used with the WUF-B connection in this study, $\theta_U = 0.047$ rad.

The WUF-B connection used in this study is shown in Fig. 2(a). The figure represents both an interior and an exterior connection. In the test specimen, exterior connections were used at the end columns and interior connections were used at the center column. As shown in Fig. 2(a), the beam web is connected to the column flange using a shear plate (shear tab), which is fillet welded to the column flange using 8 mm weld (on both sides of the plate) and bolted to the beam web using three 25 mm diameter, high strength bolts. The size of the shear tab is 13 mm × 305 mm × 152 mm. The bolt holes are standard holes with an edge distance (between the center of the hole to the edge of the shear plate) of 70 mm. The beam flanges are joined to the column flange using complete joint penetration (CJP) groove welds. Weld access holes are cut from the beam flanges in accordance with the recommendations of FEMA 350 (FEMA 2000a). Continuity plates are provided for both interior and exterior columns as shown in Fig. 2(a). No doubler plates, however, were required for either column since the shear capacity of the column in the panel zone satisfied the requirements of the AISC Specification (AISC 1999).

Reduced Beam Section (RBS) Connection

The RBS connection design resulted from extensive research following the 1994 Northridge earthquake (Chen 1996, Iwankiw and Carter 1996, Engelhardt el al. 1998). The RBS connection is created by cutting away a portion of the top and bottom flanges of the beam at a distance from the beam-column interface so that yielding is concentrated in this reduced area. The reduced section thus acts as a fuse to protect the connection against premature fracture. Various shapes of the reduced section have been suggested and studied, including straight cut sections, tapered beam sections, and circular radius cuts (FEMA 2000b). Out of the three, the radius cut section

was found to yield the most reliable performance. The RBS connection has been commonly used for seismic design since the Northridge earthquake. FEMA 355D (FEMA 2000b) provides extensive information on the testing and performance of the RBS connections under seismic loading.

The inter-story drift angle or rotational capacity of the RBS connection specified in FEMA 350 was based on a statistical analysis of the results from cyclic tests of full-scale connection assemblies. The rotational capacity corresponding to collapse prevention was estimated as:

$$\theta_U = 0.080 - 0.0003d_b \tag{2}$$

For the W24x94 beam section used with the RBS connection, $\theta_U = 0.073$ rad.

The rotational capacities in Eqs. (1) and (2) correspond to the acceptance criteria for the respective connections used in the ASCE 41-06 standard (ASCE 2007) for seismic rehabilitation of existing buildings. Although these acceptance criteria are based on seismic data, they have also been adopted by the UFC 4-023-03 guidelines (DOD 2009) for design to resist disproportionate collapse. Note that the rotational capacities in Eqs. (1) and (2) (from FEMA 350) exceed the corresponding plastic rotations presented in ASCE 41-06 (ASCE 2007) and UFC 4-023-03 (DOD 2009) by 0.01 rad, an amount approximately equal to the elastic rotation of the connections.

The RBS connection used in this study is shown in Fig. 2(b). The figure represents both an interior and an exterior connection. In the test specimen, exterior connections were used at the end columns and interior connection was used at the center column. Weld access holes were cut from the beam flanges as recommended by FEMA 350 (FEMA 2000a). Continuity plates are

provided for both center and end columns as shown in Fig. 2(b). Doubler plates were required only for the center column, based on the design calculations for the shear capacity of the column in the panel zone.

Test Program

The primary objectives of these tests are (1) to define the response characteristics of beam-column assemblies under a column removal scenario, including the capacity of the beams and their connections to carry loads through catenary action; and (2) to provide experimental data for validation of beam-to-column connection models to be used in assessing the robustness of structural systems. The following describes the overall test program, which includes test setup, loading apparatus, and instrumentation.

Test Setup

A schematic view of the test setup used for both the WUF-B specimen and the RBS specimen is shown in Fig. 3. For each specimen, the tops of the two end columns were restrained by two diagonal braces for each column, one on each side of the beam. These braces were rigidly attached to the tops of the columns and anchored to the strong floor of the test facility. The diagonal braces simulated the lateral restraint provided to the columns by the upper floor framing system in a multi-story building. Computational results presented in the companion paper (Sadek et al. 2012) show that the restraint provided by the braces produces results that are consistent with column restraint at the upper floor level. Note that such lateral restraint of the columns is necessary for the development of catenary action.

A pair of columns straddling each beam at mid-span provided lateral bracing for the beams. The vertical load was applied to the top of the center stub column by a single hydraulic

ram acting through a load cell and a steel plate. The horizontal movements of the steel plate were restrained by four columns positioned at each corner of the plate. These steel columns were welded to base plates and bolted to the test floor. A special roller bearing support arrangement at the four corners of the plate allowed free vertical displacement of the plate along the four columns. The steel plate also restrained the horizontal movements of the top of the center stub column, thereby keeping the applied load in the vertical direction and limiting eccentrically applied loading. A pair of steel plates on each side of the center stub column restrained out-of-plane motion at the lower end of the center stub column.

Loading Aparatus and Test Sequence

A hydraulic actuator with a capacity of 2700 kN and a stroke of 500 mm was used to apply a vertical downward load to the center column of the test specimens. The load was applied under displacement control at a rate of 25 mm/min. Pre-test predictions of both the WUF-B and RBS specimens indicated that the stroke capacity of the hydraulic actuator was not enough to accommodate the maximum expected vertical displacement of the center column at failure. To adjust the stroke of the hydraulic actuator, the specimen was unloaded when the actuator had extended about 450 mm. Steel blocks were inserted between the hydraulic actuator and the top of the center column, and the specimen was reloaded. Fig. 4 shows photographs of both specimens subjected to vertical displacement of the center column.

Instrumentation

The instrumentation plan for each specimen included a load cell, displacement transducers, inclinometers, and strain gages. The primary purposes of strain measurements were: (1) to compute axial forces in the beams and columns and (2) to observe experimentally the

development of catenary action in the beams. Fig. 5 shows the placement of selected instrumentation for the WUF-B and the RBS test specimens used in this paper. The reader is referred to Sadek et al. (2010) for further details. The estimated uncertainty in the measured data was ± 1 %. In addition to these digital measurements, a high-speed video camera was used to capture the failure sequence of components at the beam-to-column connection zone at the center column.

Experimental Results for WUF-B Specimen

Observed Behavior and Failure Modes

Under monotonic vertical displacement of the center column, the WUF-B specimen experienced large deflections and rotations prior to failure. A WUF-B connection to the center column failed at a vertical displacement of the center column of about 495 mm, with a corresponding beam chord rotation of about 0.081 rad, obtained by dividing the center column displacement at failure by the centerline-to-centerline beam span of 6.10 m. At that displacement, the applied vertical load was about 890 kN. The failure was characterized by the following sequence (see Fig. 6): (1) local buckling of the top flanges of the beams near the center column, (2) successive shear failure of the lowest and middle bolts connecting the beam web to a shear tab at the center column, and (3) fracture of the bottom flange near the weld access hole.

Displacement Measurements

Fig. 7 depicts the displacement profile of the beams at different load values. The figure shows that at each level of loading, the displacement profile for each beam can be approximated by a straight line, which indicates the formation of plastic hinges at the WUF-B beam-to-column connections.

Fig. 8 shows the vertical load versus the vertical displacements measured at opposite flanges of the center column [D5 and D6, see Fig. 5(a)]. As the figure indicates, the specimen was unloaded at a vertical displacement of the center column of about 457 mm to adjust the stroke of the hydraulic ram and was then reloaded again to failure. The figure shows that the assembly remained in the elastic range up to a vertical displacement of the center column of about 50 mm. After yielding, the load continued to increase gradually with increased vertical displacement of the center column until the specimen failed. The pair of load deformation curves was nearly the same, indicating that symmetry was largely maintained during the experiment. In subsequent plots, the average of D5 and D6 is used to represent the vertical displacement of the center column.

Fig. 9 shows the horizontal displacement of the end columns at beam mid-height versus the vertical displacement of the center column. In the plot, positive values signify inward displacement. The figure indicates that one displacement transducer (D10) showed an initial outward displacement followed by an inward displacement as the behavior became dominated by tensile forces in the beam (catenary action). The other displacement transducer (D1), however, maintained an inward displacement throughout the initial (flexure action) and latter (catenary action) phases of the response. The reason for this difference appears to be a slight rigid-body rotation of the specimen in the early stages of loading, possibly due to some slip in one of the connections of a diagonal brace or column end. To remove this rigid-body component, the average of the two horizontal displacement measurements was calculated and is plotted in the figure. This average is considered representative of the inward deformation of the end columns at beam mid-height and is used for comparison with the computational modeling results (Sadek et al. 2012).

Strain Measurements

Strain gages located around the test specimen provided valuable information about the response of the assembly. The reader is referred to Sadek et al. (2010) for a detailed description of the strain measurements.

Strain gages at mid-span of the beams [sections B2 and B5 in Fig. 5(a)] were used to calculate the axial forces in the beams during the test. All strains at these sections were significantly less than the nominal yield strain of the steel (about 0.2%), indicating that at mid-span the beam remained in the elastic range throughout the loading scenario. These strains were used to calculate the axial force in the beams. The axial force in the beams versus the vertical displacement of the center column is presented in Fig. 10. It can be observed that in the early stages of the response, the behavior was dominated by flexure, indicated by the slight compressive axial force in the beams. With increased vertical displacement, tensile axial forces developed in the beams and the behavior was dominated by catenary action. At the time of failure, the axial tension in the beams was about 670 kN.

Strain gage measurements from the end columns below the beams [sections C1 and C2 in Fig. 5(a)] were used to calculate the axial forces in the columns. All strains at these sections were significantly less than the yield strain of the steel, indicating that the columns remained elastic. These strains were used to calculate the axial force in the end columns. The axial force in the end columns versus the vertical displacement of the center column is presented in Fig. 11, where it can be observed that in the early stages of the response, the end columns were in compression. With increased vertical displacement and applied load, large compressive forces developed in the diagonal braces, and as a result, axial tension developed in the end columns.

Experimental Results for RBS Specimen

Observed Behavior and Failure Modes

Under monotonic vertical displacement of the center column, the RBS specimen experienced even larger deflections and rotations than the WUF-B specimen before failure occurred. In this test, the RBS specimen failed at a vertical displacement of the center column of about 851 mm, with a corresponding rotation of about 0.140 rad, obtained by dividing the center column displacement at failure by the centerline-to-centerline beam span of 6.10 m. At that displacement, the applied vertical load was about 1780 kN. The failure was characterized by the fracture of the bottom flange in the middle of the reduced section of one of the connections near the center column. As shown in Fig. 12, the fracture propagated through the web until the vertical load-carrying capacity of the assembly was depleted.

Displacement Measurements

Fig. 13 shows the displacement profile of the beam at different load values. Dotted curves connecting the measured displacements are used to represent the deflected shape of the beams, with high local curvatures near the connections reflecting the formation of plastic hinges at the reduced sections. Note that the small differences between the displacement measurements on each side of the center column indicate a slight in-plane rotation of the center column.

Fig. 14 shows the vertical load versus the vertical displacements measured at opposite flanges of the center column [D5 and D6, see Fig. 5(b)]. As the figure indicates, the specimen was unloaded twice to adjust the stroke of the hydraulic ram. Unloading occurred at vertical displacements of the center column of about 432 mm and 813 mm, whereupon the specimen was loaded again to failure. The figure indicates that the assembly remained in the elastic range up to a vertical displacement of the center column of about 50 mm. After yielding, the load continued to increase gradually with increased vertical displacement until the specimen failed. The nearly

identical load deformation curves in the plot indicate that symmetry was largely maintained during the experiment. In subsequent plots, the average of D5 and D6 is used to represent the vertical displacement of the center column.

Fig. 15 shows the horizontal displacement of the end columns at (a) the top of the columns and (b) mid-height of the beams versus the vertical displacement of the center column. In the plots, positive values signify inward displacement. The plots indicate that the end columns maintained an inward and largely symmetric displacement throughout the response. The averages of the horizontal displacements at the beam mid-height and at the column tops were calculated and are plotted in the figure as representative of the inward deformation of the end columns. These averages are used for comparison against the computational modeling results (Sadek et al. 2012).

Strain Measurements

Strain gages at sections B2 and B7 [see Fig. 5(b)] were used to calculate the axial forces in the beams during the test. All strains at these sections were significantly less than the nominal yield strain of the steel, indicating that, at these sections, the beam remained in the elastic range throughout the loading scenario. The axial force in the beams versus the vertical displacement of the center column is presented in Fig. 16. It can be observed that in the early stages of the response, the behavior was dominated by flexure with minor axial forces in the beams. With increased vertical displacement, tensile axial forces developed in the beams. At the time of failure, the axial tension in the beams was about 2450 kN.

Strain gage measurements at each end column below the beams [sections C1 and C2 in Fig. 5(b)] and on each diagonal brace [sections E1, W1, E2, and W2 in Fig. 5(b)] were used to

calculate the axial forces in the columns and braces. All strains at these sections were significantly less than the yield strain of the steel, indicating that the columns and braces remained elastic. The axial force in each end column and diagonal brace versus the vertical displacement of the center column are presented in Fig. 17, where it can be observed that in the early stages of the response, the end columns were in compression. Note that tensile forces are positive in Fig. 17(a), while compressive forces are positive in Fig. 17(b). With increased vertical displacement and applied load, large compressive forces developed in the diagonal braces, and as a result, axial tension developed in the end columns.

Discussion of Test Results

Table 1 summarizes the rotational capacities based on the two tests conducted in this study and on prior seismic test data. Rotations at peak load based on the experimental results in this study were about 0.081 rad and 0.140 rad for the WUF-B and the RBS connections, respectively. The rotational capacities of these connections based on seismic testing data are approximately 0.047 rad for the WUF-B connection, based on Eq. (1), and 0.073 rad for the RBS connection, based on Eq. 2. These results show that the rotational capacities of these connections under monotonic column displacement are about twice as large as those based on seismic test data. Contributors to this difference may include: (1) cyclic loading leads to significant degradation in the strength and stiffness of the connection, while no such degradation is expected under monotonic loading, and (2) the applied loads are resisted by different mechanisms in the two cases, with the connection in pure flexure for seismic loading but subjected to combined flexure and tension under vertical column displacement.

Table 1. Comparison of rotational capacities of WUF-B and RBS connections based on seismic data and monotonic column displacement

Connection type	Rotational capacities (rad)	
	Seismic data (FEMA 350)	Monotonic loading (this study)
WUF-B	0.047	0.081
RBS	0.073	0.140

Summary and Conclusions

This paper presented the experimental performance of beam-column assemblies with two types of moment-resisting connections under vertical column displacement. The connections considered include (1) a welded unreinforced flange-bolted web (WUF-B) connection and (2) a reduced beam section (RBS) connection. The experimental results included the observed behavior and failure modes, along with response measurements from the displacement transducers, strain gages, and load cell.

For both the WUF-B and RBS test specimens, the beam-column assembly initially remained in the elastic range at small displacements of the center column. In that early stage of the response, the behavior was dominated by flexure. With increased vertical displacement, yielding occurred at the beam-to-column connections, and axial tension developed in the beams, indicating catenary action. The axial tension in the beams increased until the connections could no longer sustain the combined bending and axial stresses, and the beam-column assemblies failed.

Failure of the WUF-B test specimen was characterized by the following sequence: (1) local buckling of the top flanges of the beams near the center column, (2) successive shear failure of the lowest and middle bolts connecting the beam web to a shear tab at the center column, and (3) fracture of the bottom flange near the weld access hole immediately thereafter.

The failure of the RBS test specimen was characterized by the fracture of the bottom flange in the reduced section of a connection near the center column. The fracture propagated through the web until the vertical load-carrying capacity was lost.

The test results showed that the rotational capacities of both the WUF-B and the RBS connections under monotonic column displacement are about twice as large as those based on seismic test data. The rotations at peak load were about 0.081 rad and 0.140 rad for the WUF-B and RBS connections, respectively, whereas the rotational capacities of these connections based on seismic test data are approximately 0.047 rad and 0.073 rad, respectively. Currently, such seismic test data form the basis of acceptance criteria for connection rotation used in the design and evaluation of structures for disproportionate collapse potential (e.g., using UFC 4-023-03). The comparison just presented shows that this approach underestimates the rotational capacities of the connections by a factor of almost two, resulting in undue conservatism in design. Experimental data under simulated column removal scenarios, such as those reported in this study, can form the basis for improved acceptance criteria in design standards and guidelines that use the alternate path method for prevention of disproportionate collapse.

Acknowledgments

This experimental study was conducted at the Engineer Research and Development Center of the U.S. Army Corps of Engineers and was supported by the National Institute of Standards and Technology, the American Institute of Steel Construction, the Air Force Research Laboratory, and the Defense Threat Reduction Agency.

References

American Institute of Steel Construction (AISC). (1999). “Load and resistance factor design specifications for structural steel buildings.” Chicago, IL.

American Institute of Steel Construction (AISC). (2002). “Seismic provisions for structural steel buildings.” *ANSI/AISC 341-02*, Chicago, IL.

American Society of Civil Engineers (ASCE). (2002). “Minimum design loads for buildings and other structures.” *SEI/ASCE 7-02*, Reston, VA.

American Society of Civil Engineers (ASCE). (2007). “Seismic rehabilitation of existing buildings.” *ASCE/SEI 41-06*, Reston, VA.

American Society of Civil Engineers (ASCE). (2010). “Minimum design loads for buildings and other structures.” *SEI/ASCE 7-10*, Reston, VA.

Chen, S.J. (1996). “A simple and effective retrofit method for steel beam-to-column connections.” *Seventh US-Japan Workshop on the Improvement of Structural Design and Construction Practices*, Applied Technology Council, Redwood City, CA.

Department of Defense (DOD). (2009). “Design of buildings to resist progressive collapse.” *Unified Facilities Criteria (UFC) 4-023-03*, Washington, D.C.

Engelhardt, M.D., Winneberger, T., Zekany, A.J., and Potyraj, T.J. (1998). “Experimental investigation of dogbone moment connections.” *Engineering Journal*, 35(4), 128-139.

Federal Emergency Management Agency (FEMA). (2000a). “Recommended seismic design criteria for new steel moment-frame buildings.” *FEMA 350*, SAC Joint Venture and FEMA, Washington, D.C.

Federal Emergency Management Agency (FEMA). (2000b). “State of the art report on connection performance.” *FEMA 355D*, SAC Joint Venture and FEMA, Washington, D.C.

Friedman, A.D., (2009). “Axial, shear and moment interaction of WT connections.” *M.S. thesis, Milwaukee School of Engineering*. Milwaukee, WI.

General Services Administration (GSA). (2003). “Progressive collapse analysis and design guidelines for new federal office buildings and major modernization projects.” Washington, D.C.

Iwankiw, N.R., and Carter, C.J. (1996). "The dogbone: A new idea to chew on," *Modern Steel Construction*, 36(1), 18-23.

Karns, J.E., Houghton, D.L., Hall, B.E., Kim, J., and Lee, K. (2007). "Analytical verification of blast testing of steel frame moment connection assemblies." *Proceedings of the Research Frontiers Sessions of the 2007 Structures Congress*, American Society of Civil Engineers, Reston, VA, CD-ROM.

Liang, X., Shen, Q., and Gosh, S. K. (2008). "Assessing ability of seismic structural systems to withstand progressive collapse: Design of steel frame buildings." Report submitted to the Building and Fire Research Laboratory, National Institute of Standards and Technology, Gaithersburg, MD.

Sadek, F., Main, J. A., Lew, H. S., Robert, S. D., Chiarito, V. P., and El-Tawil, S. (2010). "An Experimental and Computational Study of Steel Moment Connections under a Column Removal Scenario." *NIST Technical Note 1669*, National Institute of Standards and Technology, Gaithersburg, MD.

Sadek, F., Main, J. A., Lew, H. S., and Bao, Y. (2011). "Testing and analysis of steel and concrete beam-column assemblies under a column removal scenario." *Journal of Structural Engineering*, 137(9), 881-892.

Sadek, F., Main, J. A., Lew, H. S., and El-Tawil, S. (2012). "Performance of steel moment connections under a column removal scenario. II: Analysis." submitted to *Journal of Structural Engineering*.

Thompson, S.L. (2009). "Axial, shear and moment interaction of single plate 'shear tab' connections." *M.S. thesis, Milwaukee School of Engineering*. Milwaukee, WI.

List of Figures

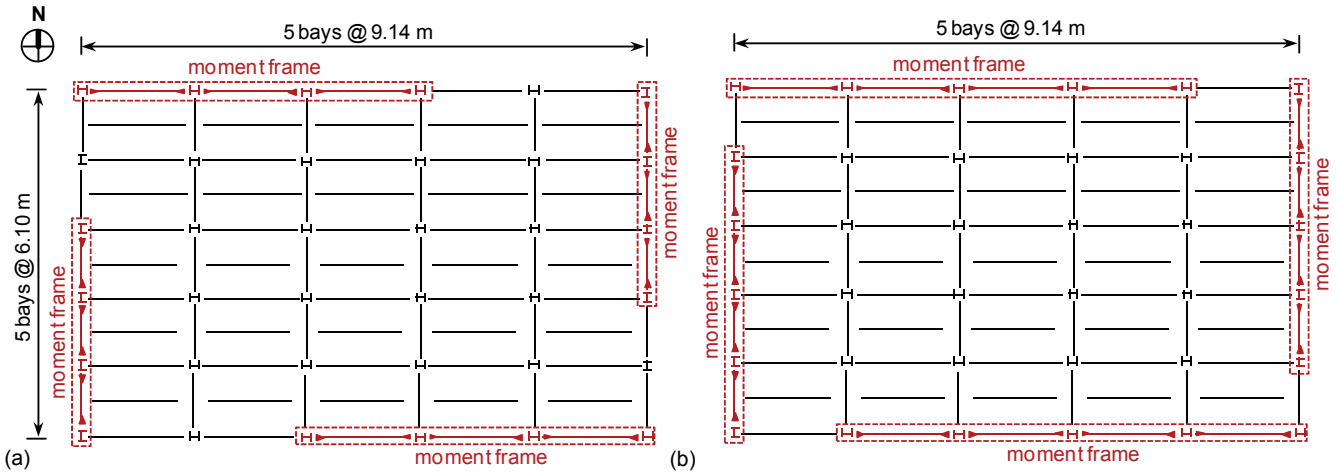

Fig. 1. Plan layouts for (a) SDC C building and (b) SDC D building

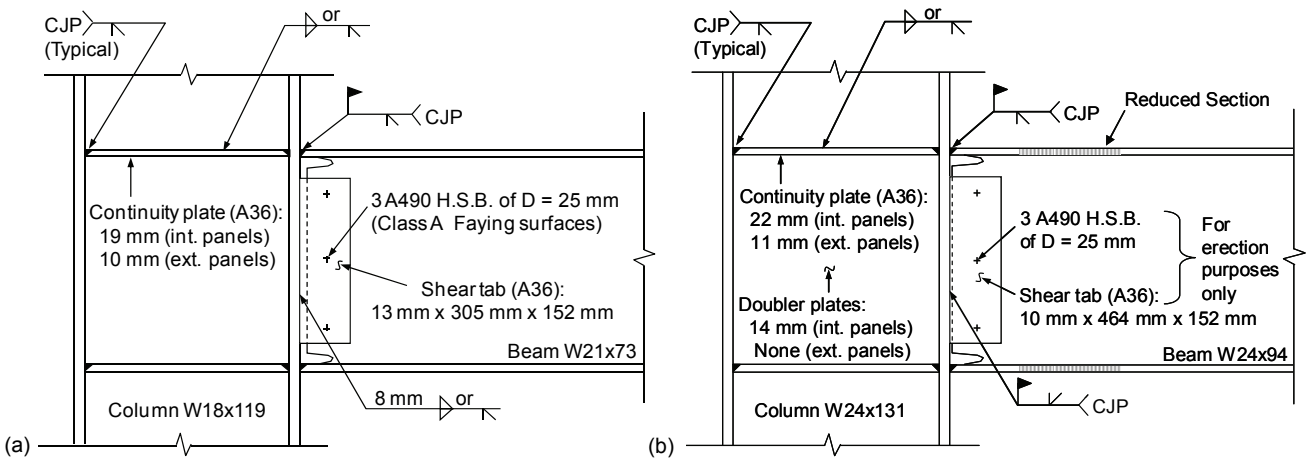

Fig. 2. Moment connection details: (a) WUF-B connection; (b) RBS connection

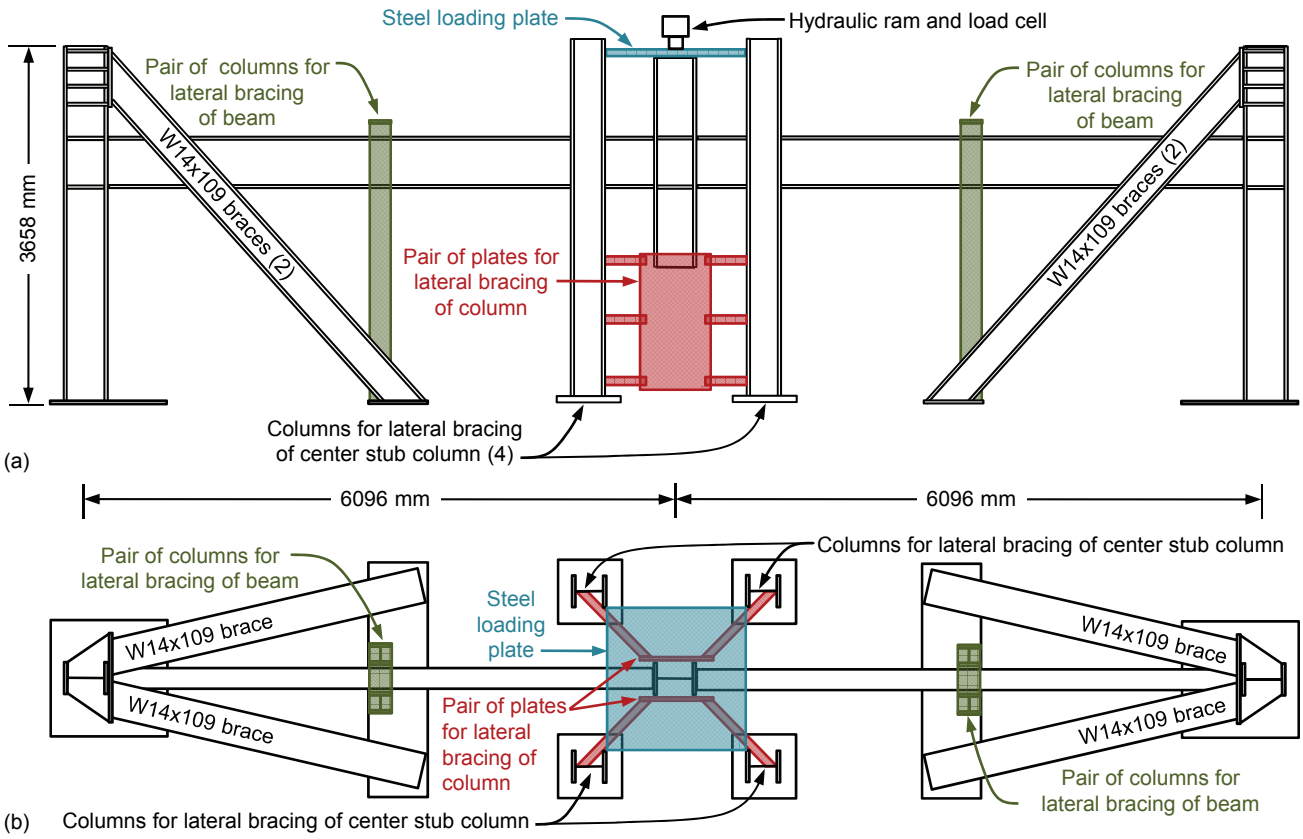

Fig. 3. Schematic of test setup: (a) elevation view; (b) plan view

(a)  (b) 

Fig. 4. Photographs of test specimens subjected to center column displacement: (a) WUF-B specimen; (b) RBS specimen

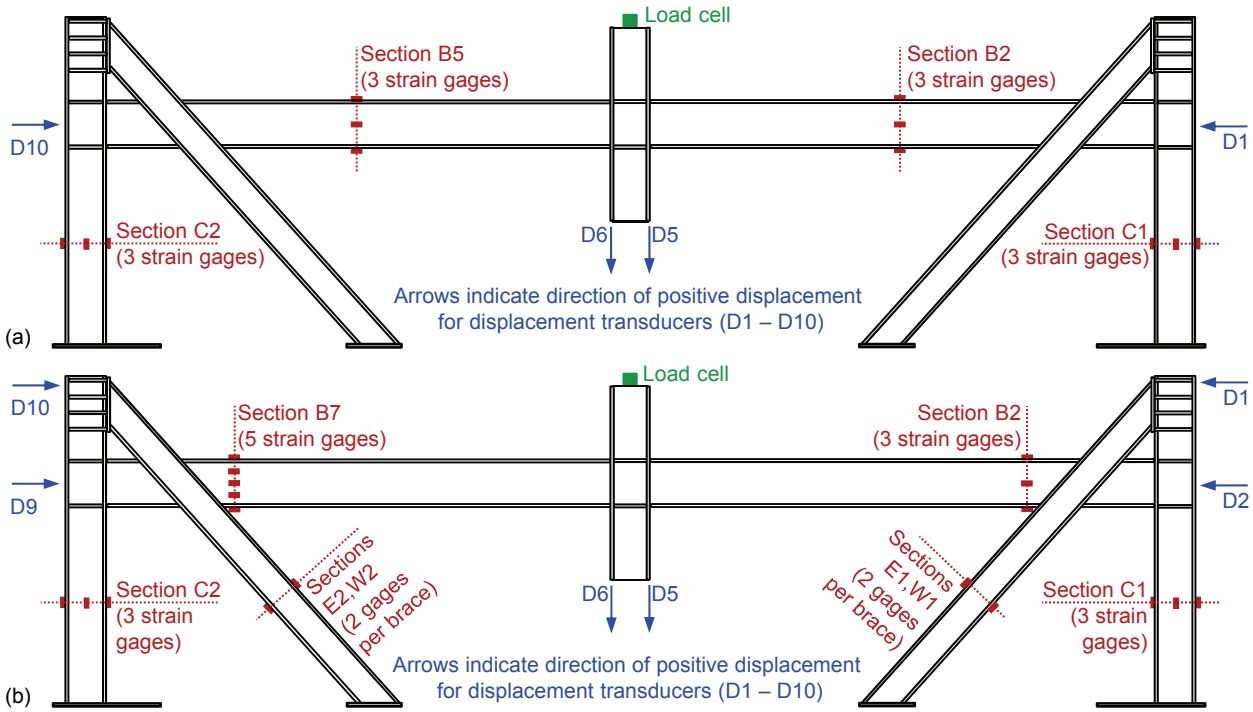

Fig. 5. Selected instrumentation for (a) WUF-B specimen and (b) RBS specimen

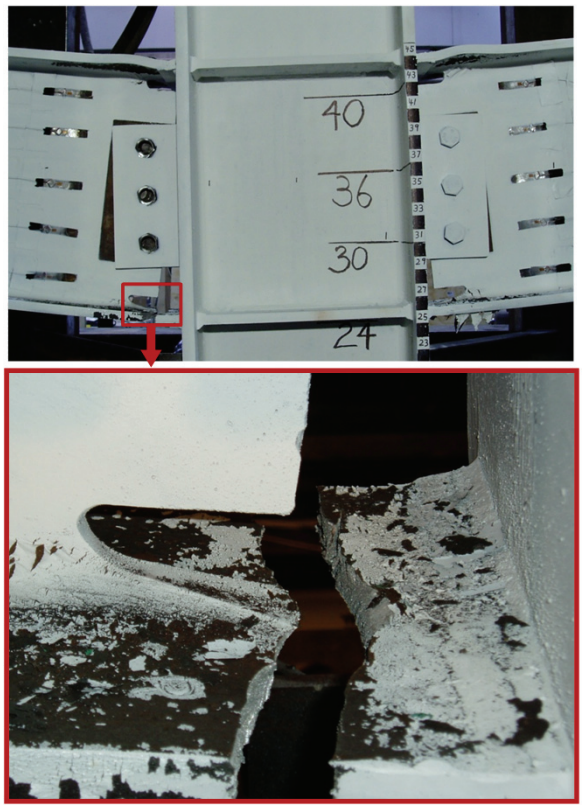

Fig. 6. Failure mode of WUF-B specimen

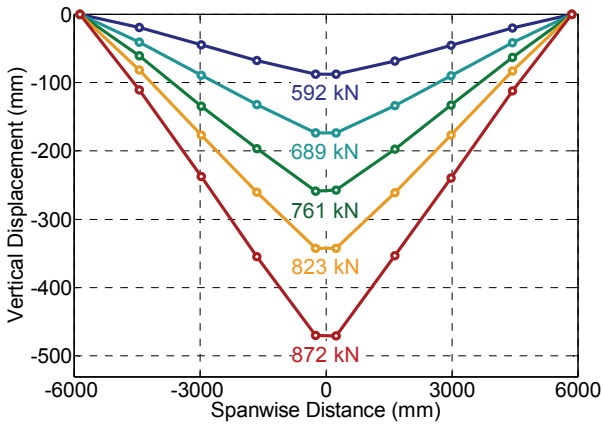

Fig. 7. Vertical displacement profile of beams corresponding to indicated vertical loads for WUF-B specimen (displacements magnified)

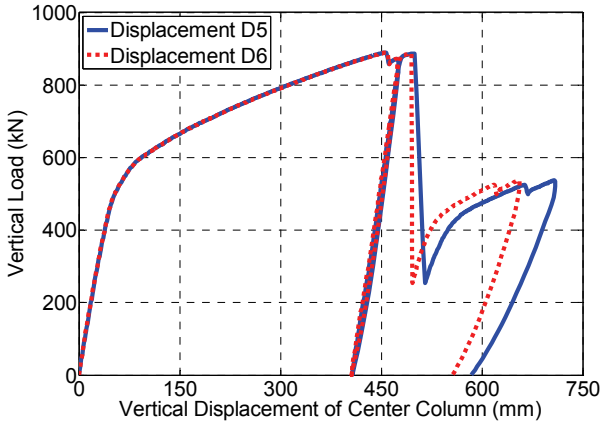

Fig. 8. Vertical load versus center column displacement for WUF-B specimen

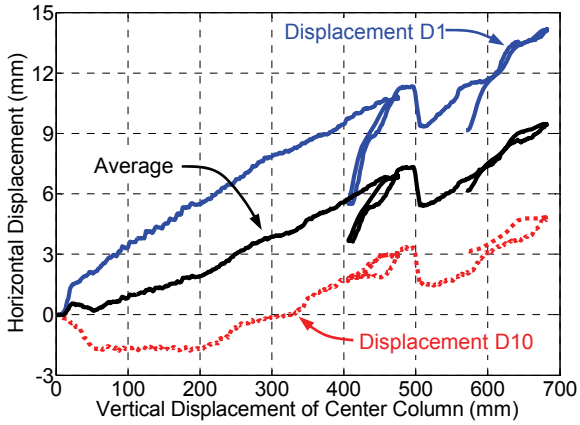

Fig. 9. Horizontal displacement of end columns at beam mid-height versus center column displacement for WUF-B specimen

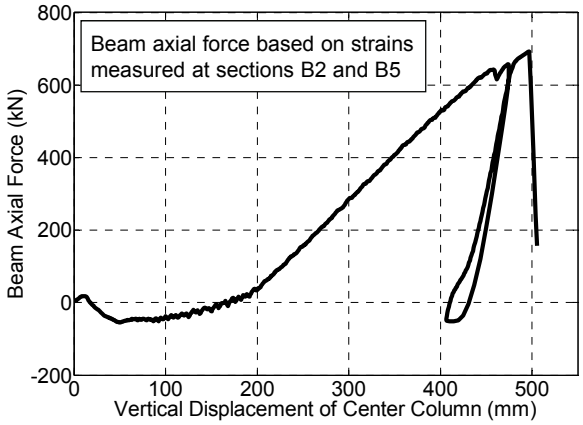

Fig. 10. Axial force in beams versus center column displacement for WUF-B specimen

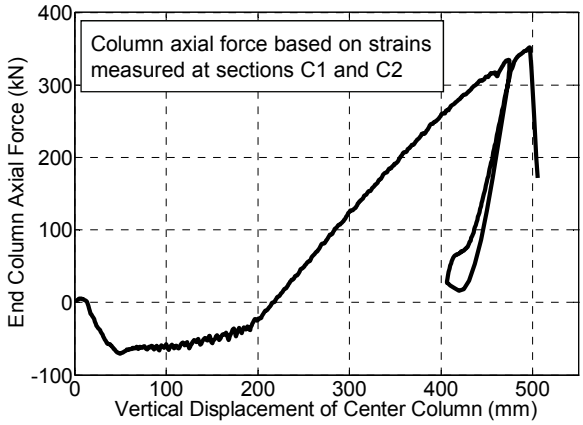

Fig. 11. Axial force in end columns versus center column displacement for WUF-B specimen

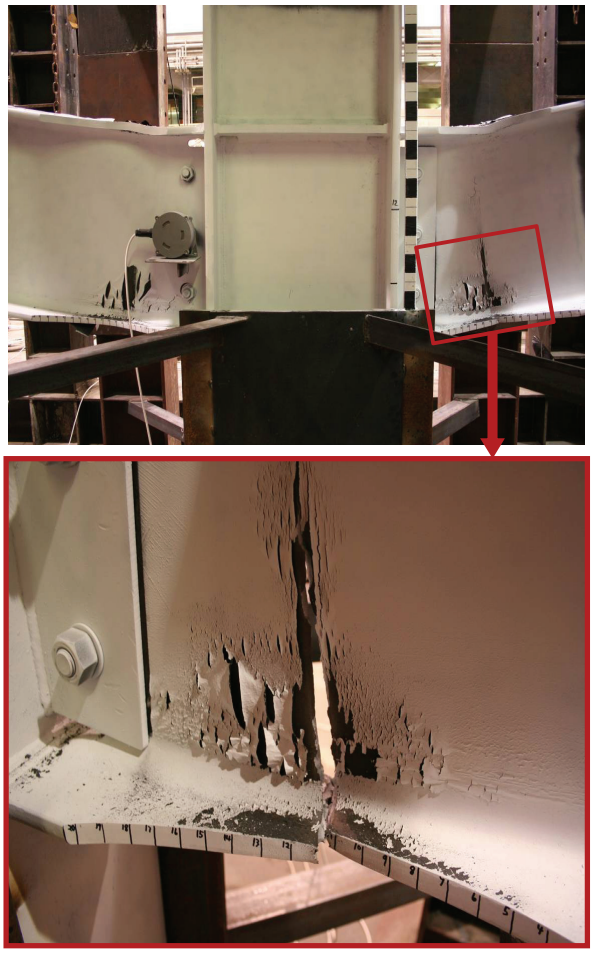

Fig. 12. Failure mode of RBS specimen

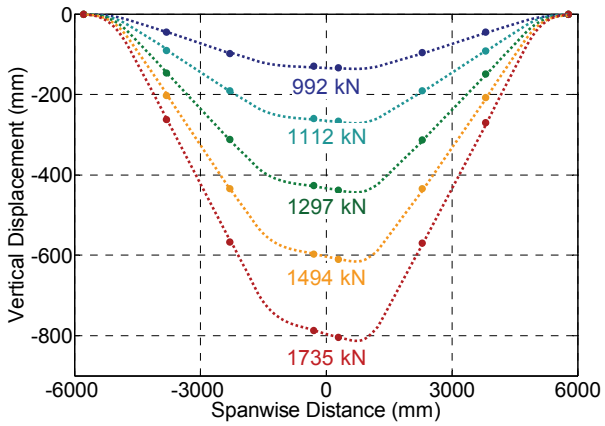

Fig. 13. Vertical displacement profile of beams corresponding to indicated vertical loads for RBS specimen (displacements magnified)

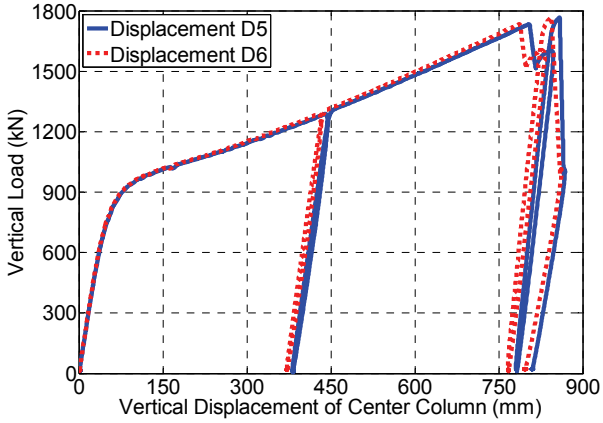

Fig. 14. Vertical load versus center column displacement for RBS specimen

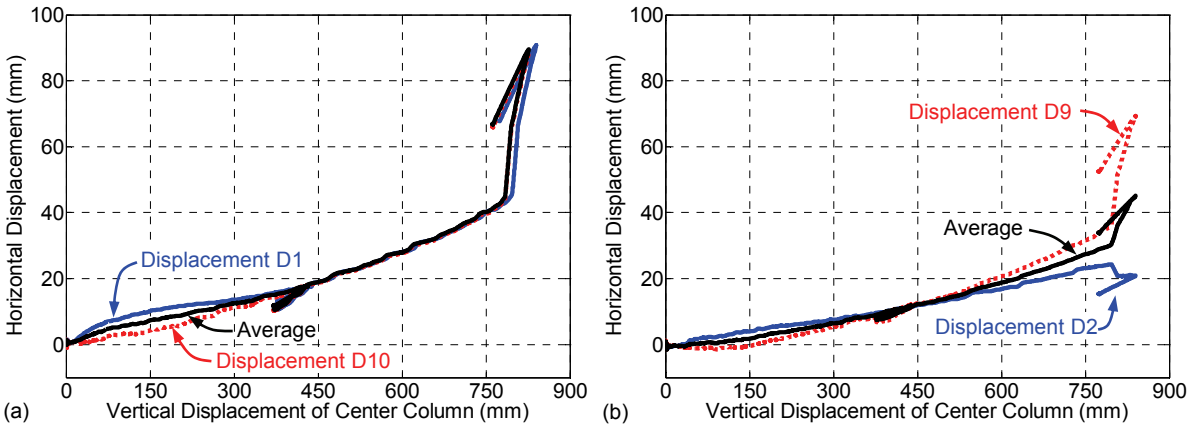

Fig. 15. Horizontal displacement of end columns at (a) top of columns and (b) mid-height of beams versus center column displacement for RBS specimen

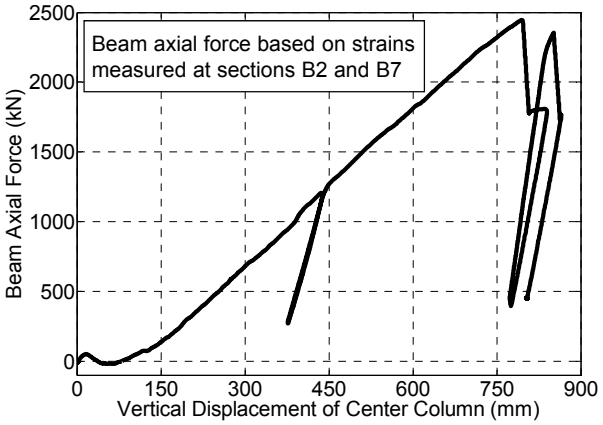

Fig. 16. Axial force in beams versus center column displacement for RBS specimen

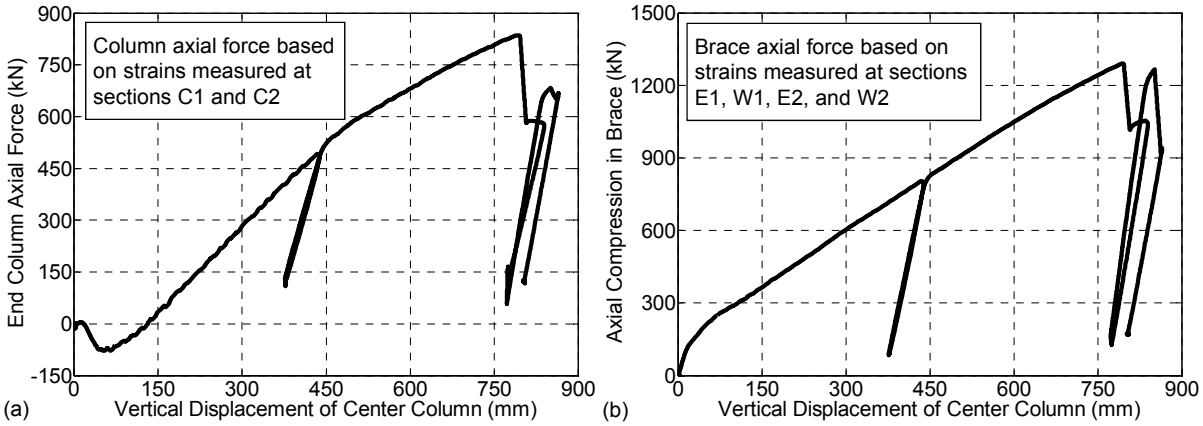

Fig. 17. (a) Axial force in end columns and (b) axial compression in diagonal braces versus center column displacement for RBS specimen